AIAA JOURNAL
Vol. 42, No. 3, March 2004

Sound Attenuation by Glow Discharge Plasma

Vadim Stepaniuk,* Valery Sheverev,† Volkan Ötügen,‡ and Calin Tarau§
Polytechnic University, Brooklyn, New York 11201
Ganesh Raman¶
Illinois Institute of Technology, Chicago, Illinois 60616
and
Vladimir Soukhomlinov**
Saint-Petersburg University, 198904, Saint Petersburg, Russia

A unique method of blocking sound waves using a glow discharge plasma sheet was demonstrated experimentally. The main thrust of the investigation was the determination of the effectiveness of using glow discharge plasma as a sound barrier in aerospace applications. Experiments were conducted in an anechoic chamber where the attenuation of single-frequency (12.5-kHz) sound propagating through a plasma sheet formed between two electrodes was studied. The sound attenuation was measured at different locations inside the chamber with the discharge plane oriented normal to the direction of sound-wave propagation. Some measurements were also carried out with the plasma plane oriented 45 deg to the sound-wave propagation direction. The measurements clearly demonstrated that the plasma attenuates sound. The highest attenuation of about 23 dB was obtained when the plasma was oriented 45 deg to the sound propagation direction. In this configuration, sound reflection from the glow discharge region was also observed. The present results suggest that the dominant mechanism responsible for the sound attenuation is the change in the index of refraction caused by gas temperature gradient at the plasma boundaries.

Nomenclature

m	=	slope of sound-pressure-level decay
n	=	electron number density
p	=	pressure
p_r	=	reference pressure
r	=	radial coordinate in cylindrical plasma
r_0	=	radius of cylindrical plasma
T	=	gas temperature
t	=	time
x	=	coordinate axis along sound propagation direction
y	=	transverse coordinate along electrode axis
z	=	transverse coordinate normal to electrode axis
α	=	sound attenuation
α_{ave}	=	spatially averaged sound attenuation
ε	=	electron energy
θ	=	sound wave incidence angle
λ	=	sound wavelength
τ	=	discharge duration

Subscript

0	=	refers to plasma axis

Presented as Paper 2003-0371 at the 41st Aerospace Sciences Meeting, Reno, NV, 6–9 January 2003; received 18 February 2003; revision received 29 September 2003; accepted for publication 2 November 2003.

*Research Assistant, Mechanical and Aerospace Engineering, Six Metrotech Center. Student Member AIAA.

†Industry Associate Professor, Mechanical and Aerospace Engineering, Six Metrotech Center.

‡Professor, Mechanical and Aerospace Engineering, Six Metrotech Center. Senior Member AIAA.

§Research Fellow, Mechanical and Aerospace Engineering, Six Metrotech Center. Student Member AIAA.

¶Associate Professor, Mechanical, Materials and Aerospace Engineering, Engineering 1 Building, 10 West 32nd Street. Associate Fellow AIAA.

**Laboratory Head, Laboratory for Novel Hypersonic Technologies, Department of Optics, Research Institute for Physics, 1 Ulianovskaja Street, Petrodvoretz.

Introduction

EXPERIMENTAL observations of the structural changes in shock waves interacting with glow discharge[1–4] have recently generated an extensive discussion in the aerospace community. Although certain inherent plasma mechanisms have been considered to explain these modifications,[5] recent experiments[6] and analysis[7] indicate that temperature gradients in the plasma formation are the primary cause for the observed wave modifications. Lately, the application of glow discharge plasma has been expanded from shock-wave studies to air vehicle drag reduction[8] and flow control.[9,10] The present research explores another potential use of plasma: the control of aeroacoustics, particularly, the containment of aircraft noise. We report on the novel use of glow discharge plasma as an acoustic barrier. To the best of our knowledge, there are no published reports that document experimental evidence of sound attenuation using a plasma barrier. Using plasma in aircraft aeroacoustics applications has the significant advantage of obtaining noise attenuation without altering the dynamics of the source. In general, noise reduction can be achieved by manipulating the source, the propagation path, or the observer. Most source alterations have aerodynamic consequences (thrust loss). At the other end, observer treatment (ear muffs or earplugs) is usually impractical. Although propagation path treatment is common in industrial situations for noise control, there has been no avenue for aircraft propagation path modification. Plasma provides this unique opportunity by allowing for the remote deposition of energy around the noise source.

For more effective utilization of glow discharges in these and other potential applications, it is important to understand the mechanism of acoustic wave interaction with plasma. Two types of mechanisms can potentially affect the propagation of acoustic waves through plasma: 1) change of wave parameters during its propagation through the plasma region itself (internal, or inherent plasma effect) and 2) reflection and refraction of the wave caused by gas temperature gradients around and inside the plasma region (boundary effect). In the plasma, the electrons absorb energy from the external electric field and deposit it into the neutral component, that is, the gas. The heating of the gas affects the acoustic wave, but the rate of energy deposition by the plasma electrons is a function of gas pressure; hence, the heating rate is affected by the propagating wave. These factors lead to a certain interaction between the acoustic wave and the plasma that can be generally described as a feedback system. This can result in dispersion, attenuation, or, in

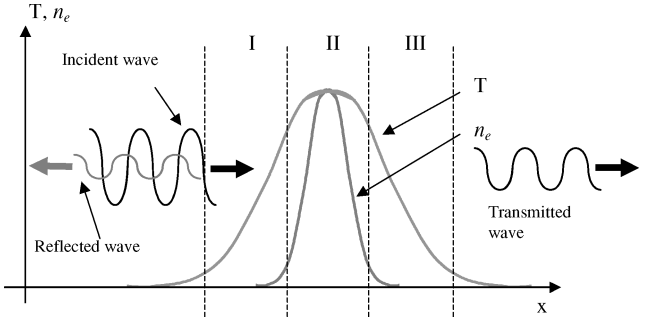

Fig. 1 Schematic representation of gas temperature and electron density distributions in the one-dimensional approximation of the glow discharge plasma.

certain conditions, amplification of the wave,[5] which essentially are internal plasma effects.

The boundary effect, on the other hand, occurs because of the difference between gas and plasma temperatures. The change in the acoustic speed (or index of refraction) in the temperature gradient zones (regions I and III in Fig. 1) between the cold gas and the hot plasma region (region II in Fig. 1) results in the reflection (and refraction) of the acoustic wave. The attenuation of the wave amplitude by this boundary mechanism can be significant particularly at large incidence angles of the wave. A one-dimensional model of sound-wave propagation through a gas with temperature gradients and reflection of sound at gas–plasma boundary was developed and presented in earlier reports.[11,12] In this paper we report results obtained through an experimental study of sound–plasma interaction.

Experimental Apparatus and Procedure

Harmonic wave reflection at the interface of two regions of different indices of refraction is known to be effective when the length of the index of refraction gradient region is small compared to the wavelength, whereas the length of each of the distinct regions is at least comparable to it. Referring to Fig. 1, this corresponds to the requirement that the length of plasma region II is equal or greater than the wavelength whereas the extent of the gradient zone I (and III) is smaller than the wavelength. Also, in order to avoid diffraction the transverse dimensions (in the directions normal to the wave propagation direction) of the barrier should exceed the wavelength significantly. These three factors prescribe the minimum dimensions for the plasma configuration and determine appropriate sound frequency range. Generating a glow discharge with transverse dimensions larger than a few centimeters at atmospheric pressure is a significant experimental challenge. It is relatively simple, however, to form an extended glow discharge ($\sim$10 cm in size) at air pressures below 100 torr. For this reason, the present experiments were conducted inside a vacuum chamber where air pressure was reduced to 80 torr. In the experiments, the transverse dimensions of the plasma were 10 and 4.5 cm while its thickness was $\sim$3 cm. Therefore, appreciable sound attenuation by the plasma should be expected for sound wavelengths smaller than 3 cm.

The experimental setup is described in detail elsewhere.[13] The main components of the setup include the vacuum chamber with a pumping and gas filling station, plasma generation system consisting of a high-voltage dc power supply, a resistor array, discharge electrodes, the sound generation and delivery system, and the sound measurement equipment. The sound measurement equipment includes a set of microphones, temperature sensors, associated electronics, as well as data acquisition and analysis hardware and software.

The cylindrical stainless-steel chamber was 87 cm long and had a diameter of 92 cm. The inside walls of the chamber were covered by wedge-type (10-cm-deep) acoustic foam to create anechoic conditions. Three optical windows allowed for visual monitoring of the discharge. A high-voltage feed-through provided a power connection to the electrodes inside the chamber. Several other ports of the vacuum chamber were used to accommodate the sound delivery tube, the pressure gauge, as well as the thermocouple and microphone leads that delivered the diagnostic signals out of the chamber.

The relative positions of the sound source, discharge electrodes, and a microphone arrangement are shown schematically in Fig. 2 along with the coordinate system. The acoustic waves originated in the center of the coordinate system. A quasi-uniform plasma was formed between the anode and the cathode. Figures 3 and 4 show the front- and side-view photographs of the plasma, respectively. The photographs were taken at an 18-deg angle to the electrode plane and axis, respectively, as indicated in the figures. Both the cathode and the anode consisted of six individual stainless-steel cylindrical sections connected to the power supply in parallel. Each cathode section was connected to the power supply in series through a 2-kΩ common and 30-kΩ individual load resistors, whereas each anode section was grounded through a 2-kΩ individual load resistor. Each electrode section was 1.6 cm long. The diameters of the anode and

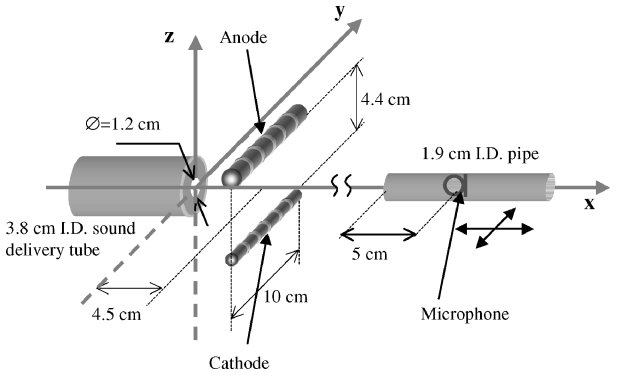

Fig. 2 Schematic of the experimental layout.

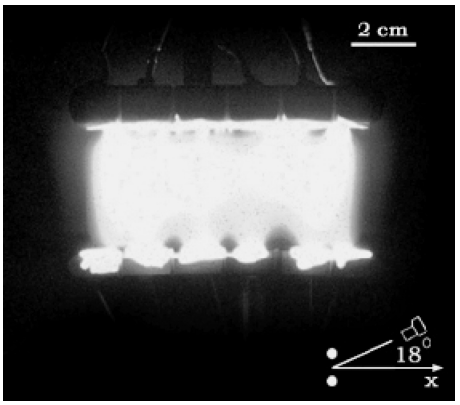

Fig. 3 Front-view photograph of the discharge.

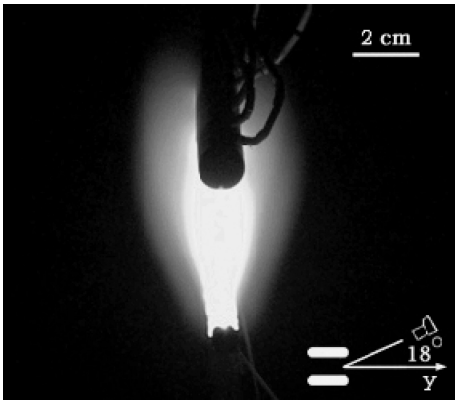

Fig. 4 Side-view photograph of the discharge.

cathode sections were 1.27 and 0.8 cm, respectively. The sections were insulated from each other using 0.8-mm-thick ceramic inserts. The total length of the electrodes was 10 cm. The electrodes were positioned 4.5 cm away from the exit of the sound delivery tube, and most of the measurements were made with the electrodes parallel to the y axis (normal sound incidence at plasma center). However, some measurements were also made with the electrodes positioned 45 deg to the y axis. In this case, the center of the plasma was 12.5 cm from the sound delivery tube exit. The z coordinate for the anode and the cathode axis were 2.8 and -2.6 cm, respectively, making the distance between the electrode surfaces equal to 4.4 cm.

The experiments were carried out with a discharge current of 0.7A, potential difference between the electrodes of 1.6 kV, and air pressure of 80 torr. The sound delivery system included a 60-cm-long, 2.5-cm-diam stainless-steel tube with a speaker chamber attached to it at one end. The other end of the tube extended into the chamber through a linear motion feed-through. A 3-in.-long ceramic tube was attached to the stainless-steel tube on the chamber end, facing the plasma in order to bring the sound output closer to the discharge and to avoid electrical breakdown through the stainless steel tube. Sound was introduced into the chamber through 1.2-cm-diam aperture forming near-spherical acoustic waves at the output of the delivery tube. Both the tube and the speaker chamber were vacuum sealed and evacuated together with the anechoic chamber throughout the experiments. The single-tone sound input was generated by a 50-W (RMS) tweeter. The tweeter was driven by a function generator through an amplifier. Several microphones (LinearX models M52 and M53) and a dynamic signal analyzer (HP 35670A) were used to measure the sound pressure levels (SPL) defined as

$$\mathrm{SPL} = 20\log(p/p_r) \tag{1}$$

where $p_r = 2 \times 10^{-5}$ Pa. The microphones were placed 5 cm deep inside $\frac{1}{4}$ in. plastic pipes to increase directivity and protect from possible electrical breakdown (see Fig. 2). During the SPL profile measurements, the microphone array was placed on a moving stage that was connected to a stepper motor, which allowed for the change of microphone position without having to open the chamber.

Before the sound attenuation measurements were carried out, several preliminary tests were conducted to qualify the experimental set up and to plan the experiment procedure. The chamber was acoustically qualified through measurements of SPL along x and y directions. In these qualification measurements the electrodes were in place, but the plasma was off. The results are presented in Figs. 5 and 6. The symbol heights in both figures represent the measurement uncertainty (one standard deviation). The SPL changes relatively smoothly in both directions, and there are no periodic structures associated with standing waves or diffraction from the electrodes. Figure 5 shows that the sound pressure level decreases with the distance from the sound source following the x^{-2} law. (A line segment with a slope of $m = -20$ is shown for reference.) The monotonic drop in the pressure levels is symmetric in the transverse y direction as shown in Fig. 6, which shows the proper alignment of the sound

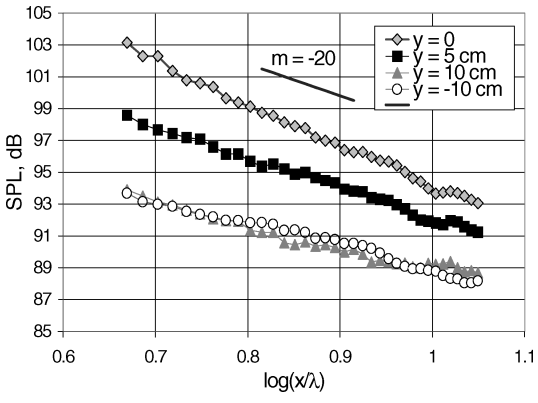

Fig. 5 SPL profiles along the x axis (at $z = 0$) for $\lambda = 2.78$ cm.

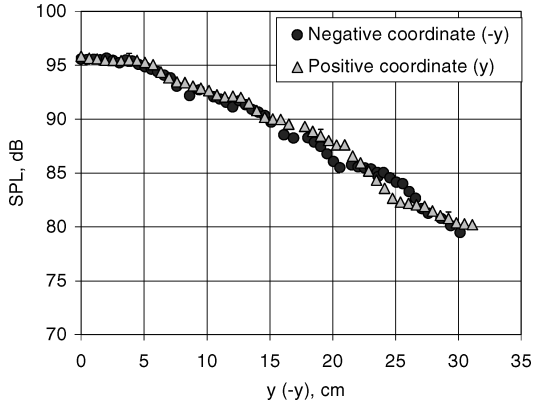

Fig. 6 SPL profile along y axis ($x = 21.5$ cm, $z = 0$).

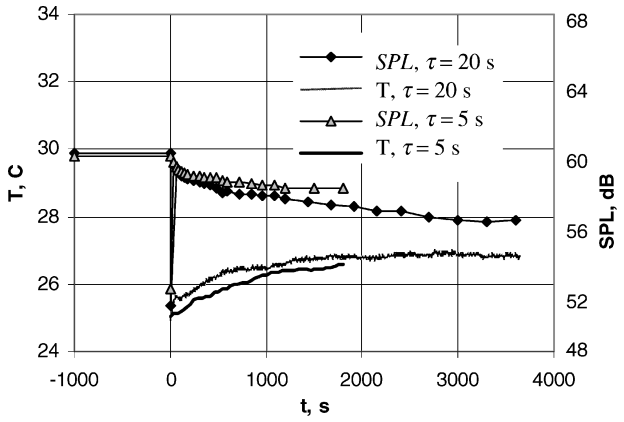

Fig. 7 Time evolution of SPL and gas temperature T measured at $x = 21.5$ cm inside the chamber for discharge durations, $\tau = 5$ and 20 s.

source and the microphone. These results combined with earlier reverberation time measurements[13] characterize the anechoic properties of the chamber as acceptable for the type of experiments presently conducted.

In the course of the experiments, it was observed that both the base sound pressure level and the attenuation by the plasma were gradually decreasing in consecutive measurements. This effect was most probably associated with continuous heating of the gas inside the chamber by repeated discharges. The temporal evolution of SPL and gas temperature in the chamber is presented in Fig. 7. In this measurement, a microphone was positioned on the x axis 21.5 cm from the electrodes, and the gas temperature was measured by a K-type thermocouple placed at the tip of the plastic cover of the microphone tube. The discharge was ignited at time $t = 0$. Two sets of measurements were made, one with discharge duration of $\tau = 5$ s and the other with $\tau = 20$ s. Immediately following the ignition of the discharge, the surrounding air was rapidly heated resulting in a significant drop in the measured sound pressure level, which is observed in the figure. A more detailed description of the SPL dynamics following the discharge ignition is given elsewhere.[13] The thermal steady state inside the chamber was established in about 30 min. The steady-state temperature was approximately 2 deg higher than the initial uniform temperature, whereas the corresponding sound pressure level was lower by 4 dB. Therefore, the rate of the heat addition into the gas had to determine the measurement cycle in the experiments. After a series of five consecutive measurements (each time igniting the discharge for no more than 5 s), the chamber was evacuated and refilled with fresh air.

Results and Discussion

The effect of acoustic frequency on the attenuation of sound by the plasma is shown in Fig. 8. For all three acoustic frequencies, the discharge current was kept at 0.5 A, and the air pressure was

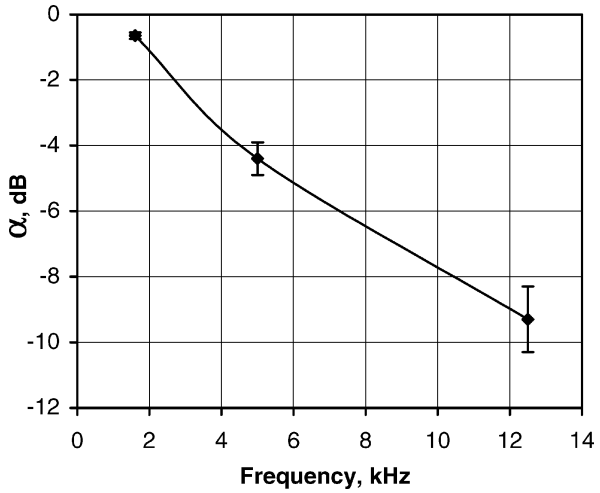

Fig. 8 Effect of sound frequency on the attenuation by the plasma (discharge current of 0.5 A).

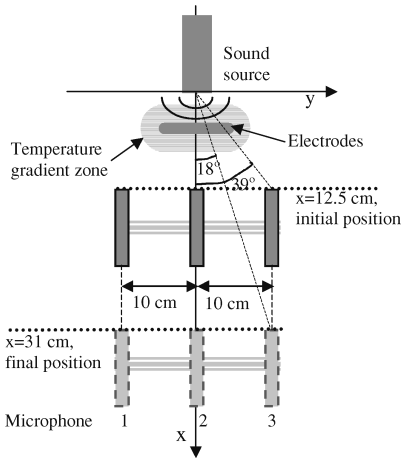

Fig. 9 Schematic of the experimental layout for attenuation measurements shown in Fig. 10

80 torr. The microphone assembly was 7 cm from the plasma. For each frequency the SPL was measured 10 times and averaged. Error bars provide the uncertainties given by the standard deviation. Each measurement was made after the plasma was established but within the next 5 s afterwards. The attenuation is a strong function of the sound frequency (or wavelength). As just discussed, for a given frequency of sound the plasma dimensions play a major role in the attenuation. Out of the three sound frequencies presented in Fig. 8, only 12.5 kHz provides the requirement that the wavelength be at least comparable to the plasma thickness and smaller than the transverse dimensions of the plasma. Therefore, in order to minimize the influence of plasma dimensions on sound attenuation the rest of the measurements discussed next were carried out at this frequency.

In the next set of experiments, the longitudinal distribution (along x) of sound attenuation was measured at three y positions. The microphone arrangement for these measurements is shown in Fig. 9. The measurements were made in the range $12.5\ \text{cm} \le x \le 31\ \text{cm}$ with an acoustic source frequency of 12.5 kHz. The three microphones were placed on the same moving stage. The electrodes were positioned parallel to the y axis and at $x = 4.5$ cm. The closest microphone position of $x = 12.5$ cm is dictated by the minimum safe distance between the microphones and electrodes, whereas the maximum distance of $x = 31$ cm is determined by the chamber length. The attenuation was calculated as

$$\alpha = \text{SPL}_{\text{plasma on}} - \text{SPL}_{\text{plasma off}} \tag{2}$$

and the results are given in Figs. 10a and 10b. Each experimental point represents the average of five separate plasma on-and-off

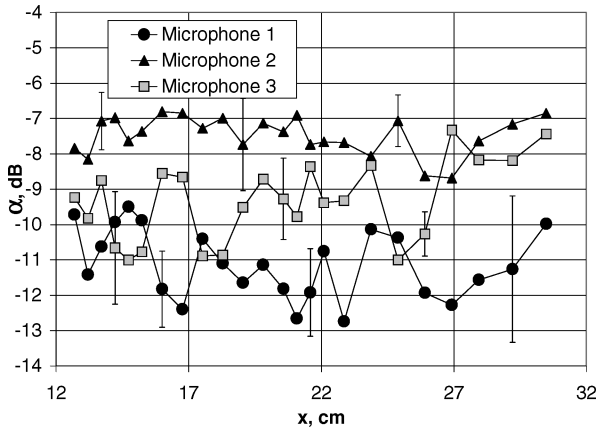

Fig. 10a Variation of α with distance x from the sound source.

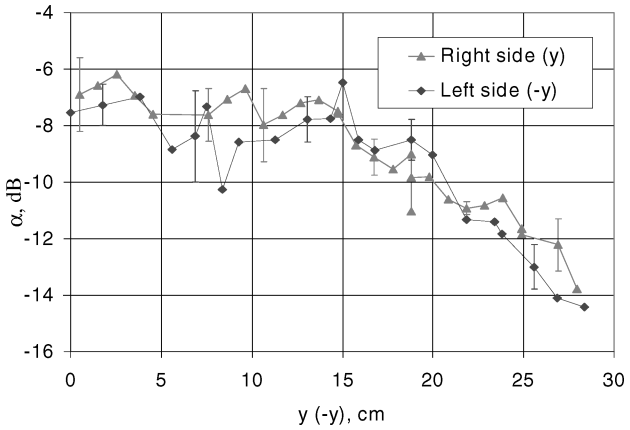

Fig. 10b Attenuation profile in y direction measured at x = 21.5 cm.

cycles, and the standard deviation of the five measurements is represented with the error bars on the graph. The attenuation measured by the center microphone (2) did not vary systematically with the distance to the sound source, staying within the range of approximately -7 to -8 dB, with an average value of -7.5 dB. This value is significantly larger than the attenuation expected because of reflection of a plane sound wave from a plasma sheet extended infinitely in the y and z directions. However, the plasma shape in this experiment cannot be approximated by a planar sheet (see Figs. 3 and 4). Sound reflection increases with angle of incidence. Also, the front of the incident waves in the experiments was clearly not planar (see Fig. 5), which takes the experimental conditions further away from the one-dimensional model. Further, the internal plasma mechanism might also have contributed to the experimentally observed attenuation levels.

The off-axis attenuations measured by microphones 1 and 3 were consistently larger than that measured at $y = 0$ by microphone 2. This is explained by the boundary reflection mechanism. For the sound-wave segments reaching the off-axis microphones, the angles of incidence on the plasma are larger than those for microphone 2, resulting in larger sound reflection. As for the two off-axis measurements, the attenuation measured by microphone 1 is stronger than that measured by microphone 3 (Fig. 10a). This is probably caused by the slight asymmetry of the discharge observed in these experiments.

The transverse profiles of sound attenuation by the discharge are shown in Fig. 10b. In this experiment a single microphone was traversed along the y axis, at $x = 21.5$ cm and $z = 0$. It is observed that sound attenuation increases with increasing lateral distance from the x axis. As the lateral distance increases, the acoustic waves are incident upon the plasma at larger angles, which results in larger sound reflection from the plasma. The attenuation profiles show good symmetry on the two sides of the x axis, which is an indication that the

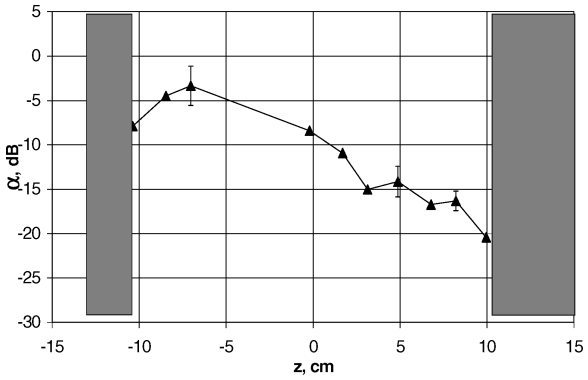

Fig. 11 Attenuation profile in z direction measured at x = 21.5 cm. (Gray areas indicate shadows from the electrodes.)

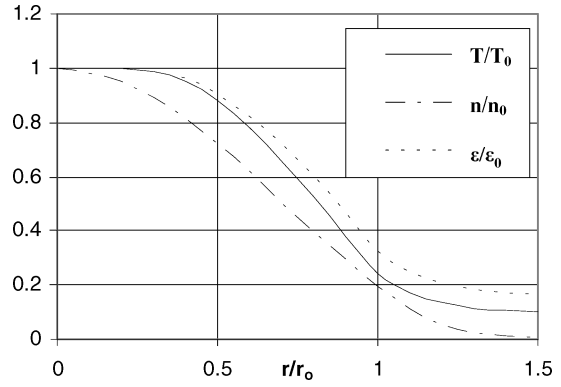

Fig. 12 Distributions of plasma properties calculated for a discharge with current density of 18 mA/cm^2 and gas pressure of 80 torr.

plasma is relatively uniform in the y direction. However, the photograph of the plasma in Fig. 4 clearly shows that the plasma is not uniform in the z direction. This is further confirmed by Fig. 11, which shows the sound attenuation profiles along the vertical direction. Unlike the y profiles, the attenuation first becomes weaker off axis in the negative z direction before it starts increasing at larger z distances. This result is consistent with Fig. 4, which shows that the thickness of the plasma near the anode is greater than that near the cathode. The effect of this asymmetry on the attenuation profile can be explained by the absorption of the wave energy in the thicker plasma layer, but it can also be explained by the boundary reflection mechanism. As just discussed, the sound reflection at the boundary of two media becomes effective when the dimension of the reflective medium along the direction of the wave propagation is larger than the acoustic wavelength. As seen in Fig. 4, the thickness of the plasma near the bottom electrode (cathode) is around 2 cm (i.e., less than the acoustic wavelength of 2.78 cm used in the experiments) while the plasma thickness near the top electrode exceeds 5.5 cm, more than twice the acoustic wavelength.

Using the attenuation profiles from Figs. 10a, 10b, and 11, we calculated a spatially averaged attenuation by integrating the SPL data over y and z coordinates as

$$\alpha_{\text{ave}} = 10\log\left(\frac{\int_{z=-10.5\text{ cm}}^{10.5\text{ cm}}\int_{y=-24\text{ cm}}^{24\text{ cm}} 10^{(\text{SPL}_{\text{plasma on}}(x=21.5\text{ cm},y,z)/10)}\,dy\,dz}{\int_{z=-10.5\text{ cm}}^{10.5\text{ cm}}\int_{y=-24\text{ cm}}^{24\text{ cm}} 10^{(\text{SPL}_{\text{plasma of}}f^{(x=21.5\text{ cm},y,z)}/10)}\,dy\,dz}\right) \quad (3)$$

which yielded $\alpha_{\text{ave}} = -7.9 \pm 0.7$ dB.

Using a recently developed one-dimensional model of an unconfined cylindrical discharge in air at pressures below 100 torr (Ref. 14), we calculated the radial distributions of the gas temperature T, electron density n, and electron energy ε for such a discharge with the plasma parameters corresponding to the present experiment (air pressure of 80 torr, discharge current density of 18 mA/cm^2). The results are presented in Fig. 12. On the discharge axis, the gas temperature, electron density, and electron energy were found to be $T_0 = 3100$ K, $n_0 = 1.27 \times 10^{10}$ cm^{-3} (this electron density corresponds to a degree of ionization of 5×10^{-8}), and $\varepsilon_0 = 3.08$ eV, respectively. The calculated characteristic discharge radius $r_0 = 1.8$ cm was found to be consistent with the thickness of the discharge used in the present experiments (Fig. 4). The plasma in the present experiments is not cylindrical or uniform in the z direction. However, the calculated spatial profiles of the plasma parameters shown in Fig. 12 should provide an adequate representation of the spatial distribution of the plasma parameters in the gradient zones.

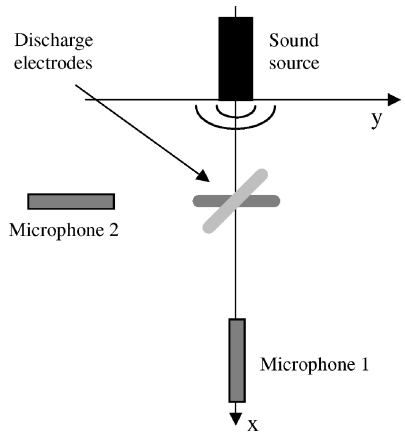

Fig. 13 Experimental layout for sound reflection measurements.

To provide a first-order comparison with the present experimental results, we calculated sound attenuation by a one-dimensional wave propagating through a high-temperature region shown in Fig. 1. The temperature gradients of zones I and III were represented by the gradient of Fig. 12, where r was replaced by x. The sound attenuation was calculated using the approach reported earlier.[11] Accounting for reflection from both sides of the slab (zones I and III of Fig. 1), we obtained an attenuation of 0.75 dB for an acoustic frequency of 12.5 kHz. This value is significantly smaller than that measured in the experiment. The difference between the calculation and measurements might be because the reflection at nonzero angles is stronger than at normal incidence, which is not accounted for in the one-dimensional calculation. Effects other than reflection on the thermal gradient boundaries (such as absorption or other type of interactions of sound wave with the plasma as it travels through the core of the discharge) might also have contributed to the discrepancy between the calculations and the experimental results.

To better determine the extent of the boundary effect, experiments were carried out to directly observe sound reflection from the plasma surface. The experimental layout is shown schematically in Fig. 13. Both microphones were placed at a distance of 14 cm from the center of the discharge. Microphone 1 was on the x axis, directly opposite to the sound source, whereas microphone 2 was normal to this axis facing directly the center of the discharge. The distance between the sound source and electrodes was set at 12.5 cm. Two sets of measurements were made. In the first, the angle between the x axis and the electrode plane was 90 deg corresponding to zero sound incidence angle upon the discharge plane. In the second, electrodes were rotated 45 deg about their midpoint in the x–y plane, providing a 45-deg incidence angle for the incoming waves. The results of the sound-pressure measurements are presented in Table 1. The sound pressure levels measured by microphone 1 demonstrate that the attenuation of the wave propagating along the x axis increases when the sound is incident upon the plasma at a 45-deg angle. When the plasma was rotated to 45 deg, the sound attenuation was -23 dB as compared to the attenuation of -10 dB at a zero incidence angle. Further, with the 45-deg

Table 1 Measured SPLs in decibels at incidence angles of $\theta = 0$ and 45 deg

	$\theta = 0$ deg		$\theta = 45$ deg	
Microphone	Plasma off	Plasma on	Plasma off	Plasma on
1	58.7	48.6	59.4	35.6
2	48.7	42.6	47.3	60.6

incident angle, the SPL measured by microphone 2 increased by 13 dB, whereas at 0-deg incidence the SPL measured by microphone 1 decreased slightly. This result provides a direct evidence for the sound-wave reflection from the plasma. Some of the increase in attenuation observed by microphone 1 for 45-deg incidence angle can be attributed to the increase in plasma thickness in the direction of sound-wave propagation. However the increase in attenuation observed seems to be too great for the ~40% change in thickness realized in the experiment. Further, it is evident from the data that a major part of the acoustic flux was simply redirected by 45-deg rotated plasma towards microphone 2. Quantitatively, the decrease of energy flux of $(4.1 \pm 0.6) \times 10^{-6}$ W/m^2, registered by microphone 1 is, within measurement uncertainty, the same as the energy flux increase of $(5.2 \pm 0.7) \times 10^{-6}$ W/m^2 detected by microphone 2. These results strongly suggest that sound reflection from the plasma boundary is the dominant mechanism of the acoustic wave attenuation by glow discharges when the thickness of the plasma in the direction of the wave propagation is comparable to the wavelength.

Conclusions

Measurements were carried out to study sound attenuation by plasma. The single-frequency sound wave at 12.5 KHz used provided a cold region wavelength of about $\lambda = 2.78$ cm, which was smaller than the transverse dimensions of the plasma and comparable to its thickness. Therefore, diffractions effects were largely avoided, whereas the thickness of the plasma was sufficient to realize sound attenuation. The measurements clearly show that the glow discharge plasma attenuates sound. It is determined that this attenuation is primarily caused by the gas temperature gradients formed at the outer edges of the plasma. Because of the rapid change in the index of refraction in the direction of sound propagation, a portion of the acoustic waves is reflected at the plasma boundary. When the sound propagates into the plasma at zero incidence angle, a spatially averaged sound attenuation of -7.9 dB is obtained. When the incidence angle is increased to 45 deg, the sound attenuation measured by the microphone directly in line with the sound source increases to about -23 from -10 dB, which further confirms that the boundary effect is the dominant mechanism of sound attenuation in the present experimental configuration. In these experiments, the relative thickness of the plasma was most likely too small to generate any possible internal plasma effect.

Acknowledgments

The authors gratefully acknowledge the support from NASA Glenn Research Center (NAG3-2533) with David W. Lam and Khairul Zaman as the Contract Monitors. We also thank Mary Jo Long Davis of NASA Glenn Research Center and Jack Wilson of QSS at NASA Glenn Research Center for their encouragement and guidance.

References

[1]Klimov, A. I., Koblov, A. N., Mishin, G. I., Serov, Y. L., and Yavor, I. P., "Shock Wave Propagation in a Glow Discharge," *Soviet Physics—Technical Physics*. Vol. 8, 1982, p. 146.

[2]Basargin, I. V., and Mishin, G. I., "Publication of the Ioffe Physico-Technical Institute," Ioffe Technical Inst., No. 880, Leningrad, Russia, Sept. 1984 (in Russian).

[3]Mishin, G. I., Serov, Yu, L., and Yavor, I. P., "Flow Around a Sphere Moving Supersonically in a Gas Discharge Plasma," *Soviet Technical Physics Letters*, Vol. 17, 1991, pp. 413–416.

[4]Ganguly, B. N., Bletzinger, P., and Garscadden, A., "Shock Wave Damping and Dispersion in Nonequilibrium Low Pressure Argon Plasmas," *Physics Letters A*, Vol. 230, 1998, p. 218.

[5]Soukhomlinov, V. S., Kolosov, V. Y., Sheverev, V. A., and Otugen, M. V., "Acoustic Dispersion in Glow Discharge Plasma: A Phenomenological Analysis," *Physics of Fluids*, Vol. 14, 2002, pp. 427–429.

[6]Ionikh, Y. Z., Chernysheva, N. V., Meshchanov, A. V., Yalin, A. P., and Miles, R. B., "Direct Evidence for Thermal Mechanism of Plasma Influence on Shock Wave Propagation," *Physics Letters A*, Vol. 259, 1999, pp. 387–392.

[7]Soukhomlinov, V. S., Kolosov, V., Sheverev, V. A., and Ötügen, M. V., "Formation and Propagation of a Shock Wave in a Gas with Temperature Gradients," *Journal of Fluid Mechanics*, Vol. 473, 2002, pp. 245–264.

[8]Roth, J. R., Sherman, D. M., and Wilkinson, S. P., "Electrohydrodynamic Flow Control with a Glow-Discharge Surface Plasma," *AIAA Journal*, Vol. 38, 2000, pp. 1166–1172.

[9]Girgis, I. G., Shneider, M. N., Macheret, S. O., Brown, G. L., and Miles, R. B., "Creation of Steering Moments in a Supersonic Flow by Off-Axis Plasma Heat Addition," AIAA Paper 2002-0129, Jan. 2002.

[10]Corke, T. C., Jumper, E. J., Port, M. L., and Orlov, D., "Application of Weakly-Ionized Plasmas as Wing Flow-Control Devices," AIAA Paper 2002-0350, Jan. 2002.

[11]Soukhomlinov, V., Stepaniuk, V., Tarau, C., Ötügen, V., Sheverev, V., and Raman, G., "Acoustic Wave Control Using Glow Discharge Plasma," AIAA Paper 2002-2731, June 2002.

[12]Tarau, C., and Ötügen, V., "Propagation of Acoustic Waves Through Regions of Non-Uniform Temperature," *International Journal of Aeroacoustics*, Vol. 1, 2002, pp. 165–181

[13]Stepaniuk, V., Tarau, C., Ötügen, V., Sheverev, V., Soukhomlinov, V., and Raman G., "Acoustic Wave Attenuation Through Glow Discharge Plasma," AIAA Paper 2002-2433, June 2002.

[14]Soukhomlinov, V., Sheverev, V., and Ötügen, V., "Distribution of Gas Temperature in an Unconfined Glow Discharge Plasma," *Journal of Applied Physics*, Vol. 94, No. 2, 2003, pp. 844–851.

G. Candler
Associate Editor